Food Chemistry: X 19 (2023) 100849

Contents lists available at ScienceDirect

Food Chemistry: X

journal homepage: www.sciencedirect.com/journal/food-chemistry-x

Fabrication and 3D printing of Pickering emulsion gel based on *Hypsizygus marmoreus* by-products protein

Dan Xu [a], Xuebing Xing [a], Bimal Chitrakar [b], Hongbo Li [a], Liangbin Hu [a], Jiayi Zhang [a], Xiaolin Zhu [a], Lishan Yao [a], Subrot Hati [c], Zhenbin Liu [a,*], Haizhen Mo [a,*]

[a] School of Food Science and Engineering, Shaanxi University of Science and Technology, Xi'an 710021, China
[b] College of Food Science and Technology, Hebei Agricultural University, Baoding 071001, Hebei, China
[c] Department of Dairy Microbiology, SMC College of Dairy Science, Kamdhenu University, Anand, Gujarat 388110, India

ARTICLE INFO

Keywords:
Hypsizygus marmoreus by-products
Protein-polysaccharide complex
Pickering emulsion gel
3D printing

ABSTRACT

Pickering emulsion gel (PEG) stabilized by the protein extracted from the by-product of *Hypsizygus marmoreus*, combining with xanthan gum (XG), was formulated as 3D printing ink. Hydrogen bonds are formed in XG/protein hybrid particles. Afterwards, PEG was developed. Results indicated that it has shear-thinning properties. The apparent viscosity, yield stress, Elastic modulus (G') and gel strength increased with the increased XG addition, while the size of emulsion decreased. XG incorporation improved the 3D printing performance with desired self-supporting capability and printing precision if its concentration reached 2.0% (w/v). This study provides ideas for the application of *Hypsizygus marmoreus* by-products protein in stabilizing PEG used for 3D printing, which has a potential to replace traditional hydrogenated cream for cake decoration.

1. Introduction

Hypsizygus marmoreus is an edible fungus with a high nutritional value, having become one of the most important varieties of edible fungi in China (Kaneko, Chihara, Shimpo, Beppu, & Sonoda, 2015; Min, Wangjinsong, Yongfa, Hui, Jianjun, & Le, 2018; Oliveira et al., 2019). In the consumption and processing, a large number of by-products (the irregular shaped mushrooms and their stalks) are usually discarded, which are similar to commercial mushrooms in terms of nutritional composition (Ingrid, Aguiló-Aguayo, Jennie, Walton, Inmaculada, Viñas, et al., 2017). However, no mature processing and reuse technology has been formed at home and abroad, resulting in a waste of resources. The by-products are rich in protein and amino acids, and are easy to digest high-quality protein with good functional properties. However, at present, the utilization rate and added value of *Hypsizygus marmoreus* protein are very low, and the high value utilization of protein resources cannot be realized.

A Pickering emulsion gel (PEG) exhibits characteristics of both an emulsion and a gel and can potentially be formulated with biocompatible and biodegradable materials, and has great potential to create and change the structure, texture and sensory properties of foods (Dickinson, 2012; Lin, Kelly, & Miao, 2020). In addition, because PEG has excellent rheological properties such as pseudo plasticity and strain resistance and certain gel strength, it can be used as a new food printing material and has application value and prospect in 3D printing (Li, Fan, Liu, & Li, 2021). Proteins play a key role in building emulsion gel systems for food 3D printing. A lot of emulsion gels based on proteins of animal origin (gelatin and whey protein) as well as proteins of plant origin (soy protein, peanut protein, etc.) have been studied (Chen, Du, Zhang, Wang, Gong, Chang, et al., 2022; Du, Dai, Wang, Yu, & Zhang, 2021; Shahbazi, Jaeger, & Ettelaie, 2022; Zhang, Jiang, Zhang, & Chen, 2022; Goldstein & Reifen, 2022). Now, the concept of health and environmental protection and the market demand for the development of new protein resources make people start to pay attention to fungus protein.

However, the emulsion gel formed only by proteins may have problems such as poor stability, weak recovery ability, and insufficient self-supporting ability, which limits its application in food 3D printing (Yu, Wang, Li, Wang, & Wang, 2022). Studies have shown that the protein-polysaccharide interaction determines the adsorption of the polymer at the oil–water interface and the affinity between the oil droplet and the gel matrix, thus affecting the microstructure, rheology and 3D printing performance of the emulsion gel (Yu, Wang, Li, Wang, & Wang, 2022). XG is a anionic polysaccharide with good emulsification, good stability and weak gelation (Russ, Zielbauer, Ghebremedhin, &

* Corresponding authors.
E-mail addresses: zhenbinliu@sust.edu.cn (Z. Liu), mohz@sust.edu.cn (H. Mo).

https://doi.org/10.1016/j.fochx.2023.100849
Received 7 July 2023; Received in revised form 10 August 2023; Accepted 23 August 2023
Available online 28 August 2023

Vilgis, 2016). The combination of protein with xanthan gum can significantly enhance the mechanical strength, elasticity and stability of emulsion gel.

In this study, protein was extracted from the by-products of *Hypsizygus marmoreus* and the possibility of PEG preparing with protein/XG composite particles was explored. The interaction between protein and XG was studied. PEG with various XG concentrations were compared and analyzed. The effects of XG on rheological behaviors, moisture state, gel strength, microstructure and 3D printing properties were investigated in order to obtain PEG with good performance and suitable for 3D printing was achieved.

2. Materials and methods

2.1. Materials

Hypsizygus marmoreus by-products were bought from Hefeng Sunshine Biotechnology Co., Ltd., Shaanxi, China. Xanthan gum (XG), in food grade, was provided by Usolf Co., Ltd, Shandong, China. Peanut oil was provided by Yihai Kerry Food Marketing Co., Ltd, Shanghai, China. Nile red and Nile blue were obtained by Shanghai Maclin Biochemical Technology Co., Ltd. Sodium hydroxide, KBr and hydrochloric acid were of analytica grade and provided by Tianjin Tianli Chemical Reagent Co., Ltd.

2.2. Hypsizygus marmoreus by-products protein extraction

The protein was extracted according to the method of Liu et al. with slight modification (Zong, Kuang, Liu, Wang, Feng, Zhang, et al., 2022). The dried by-products of *Hypsizygus marmoreus* were crushed by a mechanical mill (FW100, Xinbo Instrument Co., Ltd, Tianjin, China). Passed the powder through an 80-mesh sieve and mixed with water in 1:20 (w/v), the pH was changed to 12.0 with 1 mol/L NaOH, and they were then stirred at room temperature for 5 h and centrifuged at 8000 r/min for 20 min with the pH adjusted to 3.8 with 1 mol/L HCl for protein precipitation. The protein were collected after10 min centrifugation at 8000 r/min and washed thrice with deionized water until to neutral, followed by a freeze-drying process in a vacuum freeze dryer (LGJ-10C, Beijing, China). The protein content was determined by the Kjeldahl method to be 62.79%±1.14%.

2.3. Preparations of the Pickering emulsion gel

The PEG was prepared according to the previous method with modifications (Bi, Xu, Guo, Du, Yu, & Wu, 2022). In this study, the *Hypsizygus marmoreus* by-products protein was dispersed in deionized water to obtain required 2%, 3%, 4%, 5%, 6%, 7%, 8%, 9% and 10% (w/v) concentrations, and adjusted the pH value to 3, 5, 7 and 9. The protein solution was mixed at room temperature for 1 h, and then homogenizedby T18 homogenizer (IKA, Staufen, Germany) at 14,000 rpm for 5 min. The XG was added to the resulting protein solution with concentrations of 1%, 1.5%, 2% and 2.5% (w/v), respectively. Stir the obtained solution at room temperature for 1 h. Added Peanut oil to protein/XG mixture to obtain a mixture with oil phase volume of 40%, 50%, 60% and 70%. The mixture was then homogenizedunder 15,000 rpm for 2 min.

2.4. Amino acid composition analysis

The protein was hydrolyzed by 6 mol/L HCl, and then the amino acid compositions were determined by a HPLC system according to previous research (Girgih, Udenigwe, Li, Adebiyi, & Aluko, 2011).

2.5. Fourier transform infrared spectroscopy (FTIR)

Protein/XG mixtures were firstly freeze-dried to produce protein/XG hybrid particles. The protein/XG hybrid particles, protein and XG were elucidated by FTIR spectroscope (Frontier, Perkin Elmer). KBr were grounded with the protein/XG hybrid particles, protein and XG at the mass ratio of 100:1. Subsequently, the samples underwent the measurementin the wavenumber range of 4000 cm^{-1} ~ 400 cm^{-1}.

2.6. Gel strength

Gel strength of the PEG was analyzed with a texture analyzer (TA.XT. plusC, SMS, Britain). The mode of the measurement was selected weak gel test. The probe was selected as P/0.5R, with a pre-test, in-test and post-test speed of 2.0, 2.0 and 5.0 mm/s with 70% compression strain and 5.0 g triggering force.

2.7. Rheological properties

The rheology of the PEG was measured by a rheometer (AR-2000, TA Co., England) using a parallel plate (40 mm). The measurement spacing gap was 1000 μm. Viscosity was measured at shear rate of 0.1–100 1/s. Yield stress was determined with pressures of 0.1–2000 Pa and a frequency of 1.0 Hz. Frequency scanning was conducted with frequency of 1–100 Hz to record changes in dynamic modulus in the linear viscoelastic region.

2.8. Low-field nuclear magnetic resonance (LF-NMR)

Water movement of PEG was measured with LF-NMR analyzer (Numag Technology Co., Suzhou, China). About 3 g of the emulsion gelin the NMR tube for testing. The relaxation time was determined by the Carr-Purcel-Lmeiboom-Gill. Testing parameter was as follows: spectral width was 200 kHz, scan repetitions times were 4, wait time 1000 ms, 10,000 echoes.

2.9. Confocal laser scanning microscopy (CLSM)

Microstructure of PEG was determined by referring to the method of Shahbazi et al. (H. E. Shahbazi & Rammile, 2021) with some modifications. 2 mL Pickering emulsion gel were mixed with 40 μL of 0.1% (w/v) Nile red and 0.1% (w/v). Nile blue to stain the protein and oil. The observation of the microstructure of the samples was carried out with a CLSM (LSM800, Oberkochen, Germany).

2.10. Particle size measurement

Particle size was tested with a particle size analyzer (Malvern Instruments Ltd., Worcestershire, UK). The samples were dispersed in water, the stirring speed was adjusted to 2500 r/min and the refractive index was 1.1 for measurement (An, Liu, Mo, Hu, Li, Xu, et al., 2023).

2.11. 3D printing

A 3D Printer (FOODBOT-D1, Shiyin Co., Ltd., Hangzhou, China) was used to print according to the method of Liu et al. (Liu, Bhandari, Prakash, & Zhang, 2018). The 3D printing models were a cuboid (36.18 mm × 38.04 mm × 8 mm) and a three-dimensional five-pointed star (16 mm × 16 mm × 10 mm). The nozzle diameter was 0.8 mm, printing rate was 28 mm/s, the infill pattern was rectilinear, the infill density was 100%, and the printing was conducted at room temperature.

2.12. Statistical analysis

All tests were conducted at least three times, and the result was presented as mean ± standard deviation. Graphs were plotted using Origin 2018. SPSS software was used to analyze variance at a significance level of $p < 0.05$.

3. Results and discussions

3.1. Amino acid composition analysis

A summary of the amino acid composition of the *Hypsizygus marmoreus* by-products protein was presented in Table 1. The total amino acid (TAA) content was 32.14 g/100 g, and the essential amino acid (EAA) was 15.7 g/100 g, accounting for 0.49 of the TAA, which was higher than the recommended value of 0.4 by the FAO/WHO (Millward, 2012). The contents of Thr, Val, Ile, Leu, and His in the protein were 1.47, 2.28, 2.00, 3.94, and 1.86 g/100 g, respectively, which were higher than the recommended adult requirements by FAO/WHO (Organization, 1991). In addition, the content of Phe + Tyr was 3.64 g/100 g, which exceeded the recommended value of 1.9 g/100 g. Therefore, the *Hypsizygus marmoreus* protein is expected to be a high-quality protein resource.

3.2. FTIR

The structures of protein, XG, and protein-XG composites were analyzed by FTIR (Fig. 1). The characteristic peaks at 1731 cm^{-1} and 1618 cm^{-1} of XG corresponded to the stretching vibration of C═O and COO–, respectively (Bi, Xu, Guo, Du, Yu, & Wu, 2022). The specific absorption peaks of protein appeared at 1654 cm^{-1} and 1538 cm^{-1}, which were explained to the stretching vibrations of C═O and C=N (amide I), the deformation vibrations of C—N and N—H (amide II) (Sow, Chong, Liao, & Yang, 2018). The protein had a strong absorption peak at 2925 cm^{-1} by the stretching vibrations of = C—H and $–NH^{3+}$ in amide B, which may be attributed to the strong hydrophobicity (Chang, Chao, Xue, Jingyi, Wang, Taoran, et al., 2017). After adding XG, the intensity of the peak at 2922 cm^{-1} of the protein-XG composite decreased, indicating a decrease in hydrophobicity (Chang et al., 2017). XG has a broad absorption peak at 3563 cm^{-1}, which was assigned to the stretching vibrations of –OH, indicating its certain hydrophilicity (Huang, Wang, Ahmad, Ying, & Tan, 2021). Meanwhile, the hydrophilic peak of protein appeared at 3289 cm^{-1}. After the formation of the protein-XG complex, the peak at 3289 cm^{-1} shifted to 3362 cm^{-1}. These results indicated that hydrogen bonds were formed between the amide groups of protein and the hydroxyl groups of XG. The similar phenomenon was observed in FTIR of pecan protein/xanthan gum complex (Li, Huang, Zhang, Chen, & Huang, 2020), indicating the occurrence of physical aggregation in the protein-XG composite.

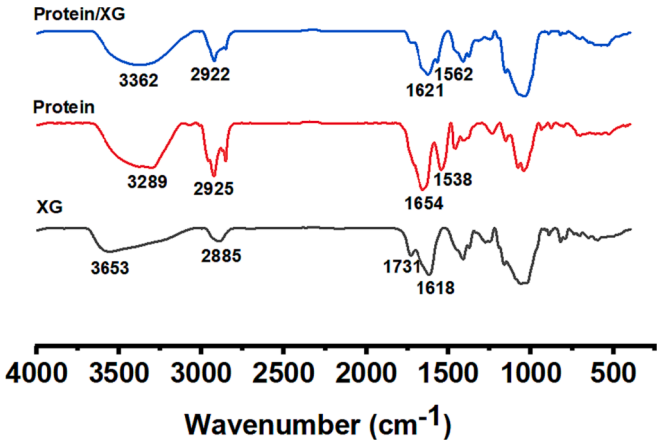

Fig. 1. Fourier Transform infrared spectroscopy analysis.

Table 1
Amino acid composition of *Hypsizygus marmoreus* by-products protein.

Amino acid	Content (g/100 g)	FAO/WHO recommended value (adult requirement, g/100 g)
Asp	3.40	
Thr*	1.47	0.9
Ser	1.36	
Glu	3.89	
Gly	1.87	
Ala	2.28	
Cys	0.05	
Val*	2.28	1.3
Met*	0.57	
Ile*	2.00	1.3
Leu*	3.94	1.9
Tyr*	1.31	
Phe*	2.33	
His*	1.86	1.6
Lys*	1.25	1.6
Arg	0.66	
Pro	1.62	
TAA	32.14	12.7
TEAA	15.7	15.7
TEAA/TAA	0.49	0.4

Total amino acids - (TAA);
* Total essential amino acids - (TEAA).

3.3. Formation and characterization of Pickering emulsion gel

Firstly, the visual appearance and storage stability of Pickering emulsions stabilized by 2% to 10% (w/v) protein with the oil volume fractions of 40%-70% and pH ranging from 3 to 9 were characterized. The influences of protein concentration on samples were studied with 50% oil volume fraction and pH 7 (Fig. 2A). From the appearance, regardless of the protein concentration, the freshly prepared Pickering emulsion was uniform, but exhibited diverse states occurred during storage. The extensive water eluting and oiling off occurred in the Pickering emulsion stabilized by 2% to 7% (w/v) protein. With the increased of protein concentration, the phase separation was improved and the amount of separated water decreased. When the protein concentration reached 8% (w/v), the oiling off was mainly observed. When the protein concentration reduced, the oil–water interface cannot be completely covered by the protein, resulting in phase separation of Pickering emulsion. At high protein concentration, there were enough particles to form a dense interfacial film at the oil–water interface, resulting in improved stability. However, when the protein concentration was higher than a certain range, the protein accumulated in the lower layer and oiling off was occurred (Li, Liu, Xu, & Zhang, 2022).

The influences of oil volume fraction (40%-70%) on Pickering emulsion were explored with a protein concentration (7% (w/v)) and pH 7, as shown in Fig. 2B. As the oil volume fraction increased from 40% to 70%, the emulsion gradually showed a clear oil phase. This was because amounts of protein particles were insufficient to cover the interface and flocculation occurred with the increase of oil volume fraction, resulting in oil–water phase separation (Palazolo, Sobral, & Wagner, 2011). The emulsion formation was also investigated under different pH range of 3.0–9.0. As shown in the Fig. 2C, at pH 3.0, some water separated from the emulsion. At pH 5.0, a significant amount of oiling off was occurred. The emulsion prepared at pH 7.0 was homogeneous. When pH was 9.0, flocculation appeared in the emulsion.

The Pickering emulsion prepared with protein particle stability was not suitable for 3D printing, so in the following study, XG was added under the condition of 7% (w/v) protein concentration, 50% oil volume fraction and pH of 7 to convert the Pickering emulsion into PEG. The emulsion gels prepared at different XG concentrations (0–2.5% (w/v)) were further analyzed and 3D printed. Fig. 3A showed the appearance and inversion experiment of emulsion gels prepared under different XG concentrations. The PEGs stabilized by protein/XG passed the inversion test. In contrast, the PEGs remained stable with higher XG concentrations (1%-2.5% (w/v)), which could keep on the top of the upside down bottles. This showed that the gel network structure was formed after XG was added, and the gel strength was improved.

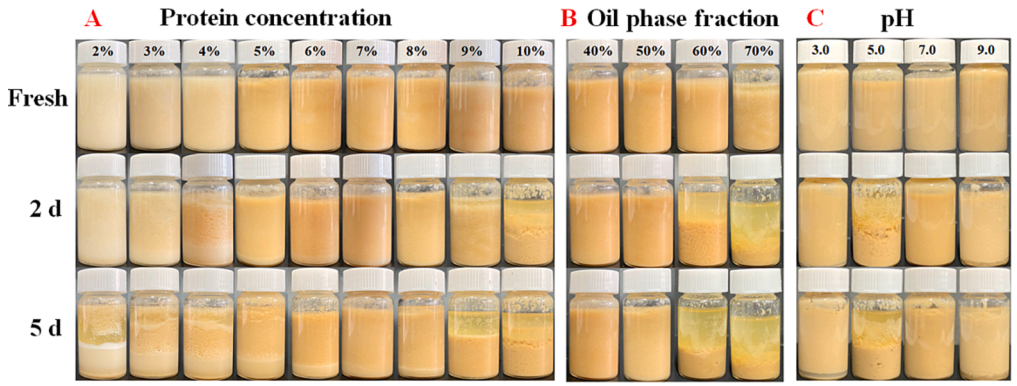

Fig. 2. The Pickering emulsion gels prepared at different conditions. A: Pickering emulsion gels prepared at different protein concentration (2%-10% (w/v)) at pH 7 with 50% oil phase fraction; B: Pickering emulsion gels prepared at different oil phase fraction (40%-70%) at pH 7 with 7% (w/v) protein concentration; C: Pickering emulsion gels prepared at different pH (3–9) with 7% (w/v) protein concentration and 50% oil phase fraction.

3.4. Gel strength

The gel strength of samples was shown in Fig. 3B. The sample without XG appeared liquid, and the gel strength could not be measured, so it was not shown in the figure. The gel strength of the emulsion gel increases from 30.67 g to 130.21 g with the increase of XG content from 1.0% to 2.5% (w/v). This was possibly because the addition of XG increased the flocculation bridge between adjacent droplets and formed a network structure (Liu, Xu, & Guo, 2007). With the increase of XG concentration, the network formed was stiffer, and the gel strength of Pickering emulsion gel was stronger (Patel, Cludts, Sintang, Lesaffer, & Dewettinck, 2014).

3.5. Rheology of Pickering emulsion gel

The apparent viscosity of the PEGs was explored using the shear scan test (Fig. 3C). The apparent viscosity of each sample reduced when the shear rate increase, indicating the shear-thinning behavior of the samples, which may be related to the destruction of droplet clusters under shear stress (Liu, Zhang, Wang, Bao, & Zhou, 2019). The shear-thinning behaviour of the emulsion gel facilitates its extrusion from the printer nozzle (Xing et al., 2022). The viscosity of samples increased with the increase of XG concentration. When no XG was added, the initial viscosity of the sample was 16.15 Pa.s, and with increasing XG concentration up to 2.5% (w/v), the initial viscosity of the sample increased to 431.46 Pa.s. This is due to the participation of XG in the formation of the gel network in the emulsion gel, enhancing the mechanical properties of the emulsion gel and increasing the apparent viscosity (Imeson & Alan, 2009).

Yield stress of each sample was obtained through stress sweep tests (Liu, Bhandari, Prakash, Mantihal, & Zhang, 2019). As shown in Fig. 3D, with increasing XG concentration, the yield stress of the emulsion gel gradually increased. When no XG was added, the prepared emulsion was in a liquid state, and its yield stress was 1.77 Pa. With the XG concentration increased from 1.0% to 2.5% (w/v), the yield stress of the emulsion gel increased from 30.67 Pa to 130.21 Pa. Again, this was probably due to the ability of XG to crosslink proteins, forming a gel network in the emulsion, and the PEG with higher added XG concentration formed a stronger network structure than the Pickering emulsion gel with lower added XG (Huang et al., 2021; Liu, Xu, & Guo, 2007).

The viscoelasticity of PEG was determined by frequency scanning. As shown in Fig. 3E, the G′ was always greater than G″ at 1 ~ 10 Hz for all samples, indicating the elastic semi-solid characteristics (Hinderink, Schröder, Sagis, Schroën, & Berton-Carabin, 2021). Additionally, the viscoelasticity of the sample is related to the self-supporting ability of the 3D printed structure (Liu, Bhandari, Prakash, Mantihal, & Zhang, 2019). G′ increased with increasing XG concentration over the studied frequency range, again indicating that the addition of XG improved the mechanical strength of the PEG (Mezger, 2020). This was because XG forms a firm gel network in the emulsion, and the higher the concentration of XG, the stronger the gel strength of the emulsion gel (Liu, Xu, & Guo, 2007). This indicated that the addition of XG improved the mechanical strength of the Pickering emulsion gel, which was conducive to the shape maintenance of the samples after 3D printing.

3.6. LF-NMR

Fig. 4A showed T_2 distributions of resulting PEGs displayed. The peak (T_{21} and T_{22}) occurring in the 0–10 ms indicates water that is tightly bound to the polymer and has low mobility. T_{23} and T_{24} are in the range of 10–100 ms, which represents weakly bound water, and T_{25} (100–1,000 ms) represents free water with high mobility (Zhang, Li, Li, & Liu, 2019). The peak around 100 ms has the largest proportion and has a significant impact on the rheological properties of the emulsion gel (Liu, Zhang, Bhandari, & Wang, 2017). It can be seen that as the concentration of XG increased, the relaxation time corresponding to the peak around 100 ms decreased, indicating a decreased in water migration rate and mobility. This may be attributed to the formation of a more compact network structure in the emulsion gel matrix due to the addition of XG, which enhanced the binding effect on water. This further confirms that the viscosity and G' of the PEG increased with the addition of XG.

3.7. Morphology of the Pickering emulsion gel

Fig. 4C showed the microstructure of PEG. The oil phase was in green, while the protein/XG complex was in red. The emulsion drops of PEG were embedded into the gel matrix. The oil phase was located inside the droplets, and the droplet surface was covered with protein and XG, while the rest of the protein and XG interact to form the gel network structure. The droplet size gradually decreased with the XG concentration increased, and the distribution of droplets became more uniform. This was because the crosslinking interaction between external polymer chains of the droplets was enhanced with the increase of XG, resulting in a more compact structure. A similar result was observed in tea protein/XG stabilized Pickering emulsion (An et al., 2023). When the XG concentration is 2.0% and 2.5% (w/v), the droplet size is smaller, and each droplet can be fully coated by the protein/XG polymers around it. The smaller droplet size and the network structure of polymers around the droplets can enhance the stability of the emulsion (Huang et al., 2021). In addition, the appearance of all samples did not show phase separation, and the surface of the emulsion gel was more delicate. After adding XG, all the PEGs prepared passed inversion test. This indicates that the gel network structure was formed after the addition of XG, which

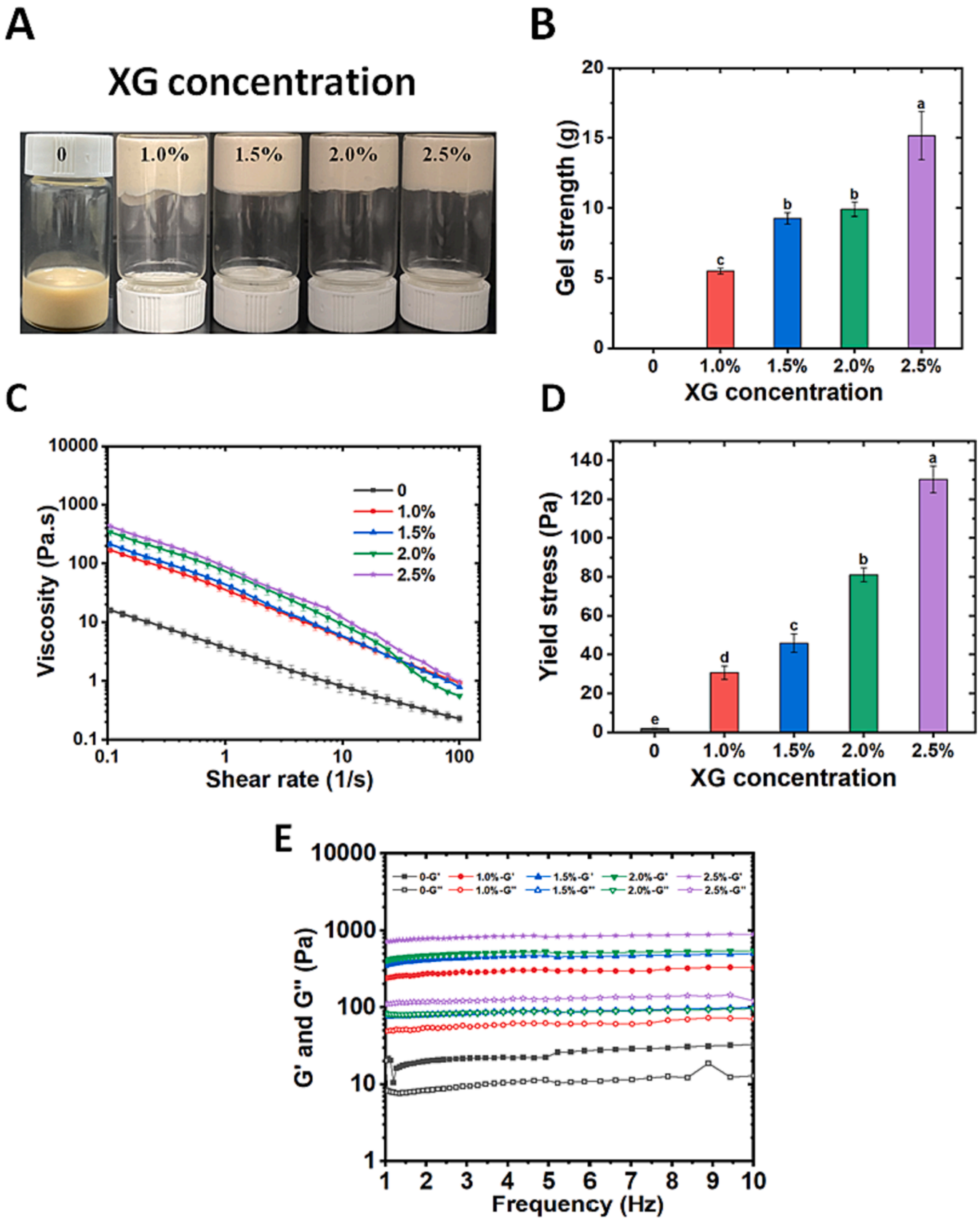

Fig. 3. A: Pickering emulsion gels prepared at different XG concentration (0–2.5% (w/v)); B: The gel strength of Pickering emulsion gels prepared with different XG concentrations; C: Shear scanning test of Pickering emulsion gel; D: Yield stress of Pickering emulsion gel; E: Frequency sweeping test of Pickering emulsion gel.

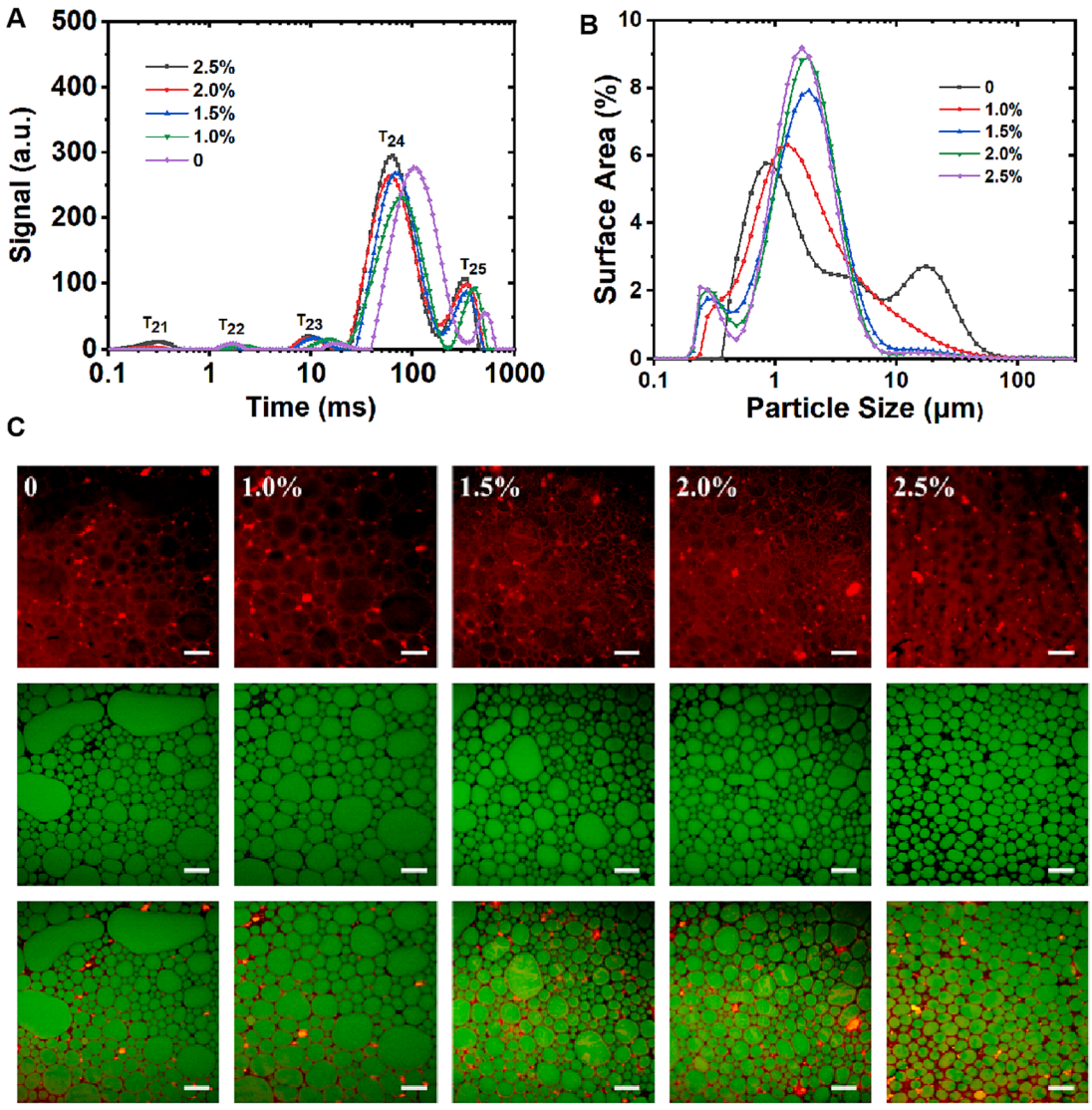

Fig. 4. A: Effects of XG concentrations on the water distribution of Pickering emulsion gel; B: Particle size distribution of Pickering emulsion gel prepared with different XG concentrations; C: CLSM of Pickering emulsion gel at different XG concentrations.

affected the texture and rigidity of the PEG.

3.8. Particle size distribution of Pickering emulsion gel

The particle size of PEG was shown in Fig. 4B. The particle size distribution of emulsion exhibited a bimodal distribution within the range of 0.1–100 μm without XG, indicating that the emulsion was not uniformly dispersed. As the XG concentration increased, the particle size distribution curve shifted to the left, and the peak became narrower, indicating that the droplets were more uniformly dense (Taha, Ahmed, Ismaiel, Ashokkumar, Xu, Pan, et al., 2020). When the XG concentration increased from 1.0% to 2.5% (w/v), the droplet size gradually decreased. This was because as the protein /XG increased, there were enough particles to cover the oil–water interface, reducing the interfacial tension and form smaller emulsion droplets (Lin, Meng, Yu, Wang, Ai, Zhang, et al., 2021). Researchers have shown that a reduction in droplet size could enhance the interaction between emulsion droplets, thereby increasing the viscosity and stability of the PEG (Derkach, 2009). Therefore, the viscosity and stability of the Pickering emulsion gel also increased with the XG increased.

3.9. Application in 3D printing

As shown in Fig. 5, without the addition of XG, the sample remained in a liquid state after printing and cannot be printed into a desired shape, which is consistent with the results from rheological and gel strength experiments. When the XG concentration was 1.0% (w/v), the PEG could be smoothly extruded through the printing nozzle and printed according to the design model, but the printed product gradually collapsed and fused together. This was because the addition of XG increases the G′ and gel strength of the PEG, but 1.0% (w/v) XG was not sufficient to support a stable structure. As the XG concentration increased to 1.5% (w/v), the layers of the printed samples become apparent, and the shape of the samples approaches the design model, but the samples still sink slightly due to insufficient mechanical strength to support the structure. When the XG concentration was 2.0% (w/v), the prepared PEG could be printed into a stable structure and the shape of the printed products were consistent with the design model, with clearer textures. When the concentration of XG was 2.5% (w/v), the product with high printing accuracy could also was obtained, and the stability was relatively higher. In general, when the XG concentration was 2% and 2.5% (w/v), the 3D printing effect was similar. This was mainly due to the fact that after the XG concentration reached 2% (w/v), the PEGs

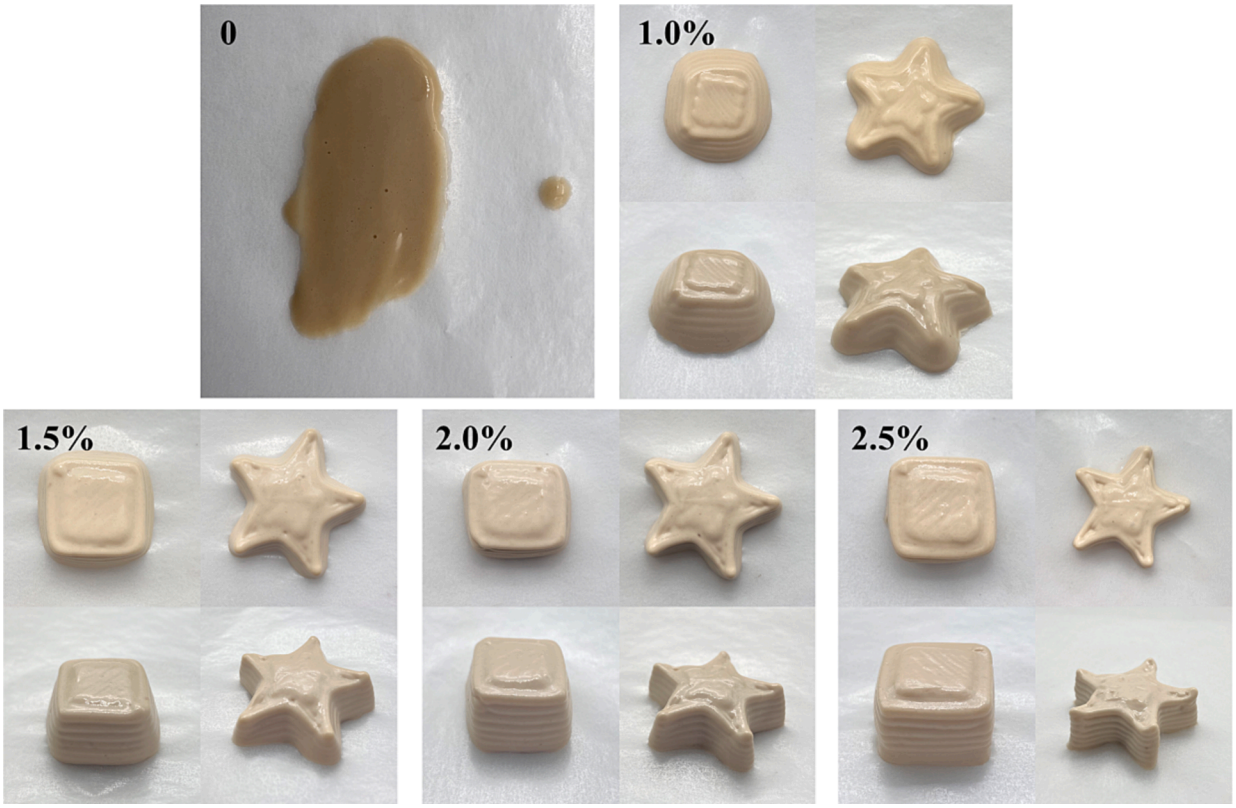

Fig. 5. Pickering emulsion gel with different XG concentrations was printed different three-dimensional structures (The printing time of cuboids was 7 min 22 s; the printing time of three-dimensional five-pointed stars was5 min 57 s).

had the suitable printing characteristics, making the extrusion line clearer, and had the appropriate mechanical strength, making it able to support the structure stable.

4. Conclusion

In this study, natural proteins were obtained from the *Hypsizygus marmoreus* by-products. PEG stabilized by the proteins and XG were prepared. The results showed that hydrogen bonds were formed between the by-product protein and XG. The prepared PEG had shear-thinning characteristics. With an increase in XG concentration, the apparent viscosity, yield stress, G′, and gel strength of the emulsion gel increased, indicating that XG participated in the formation of the gel network and improved the gel strength. The addition of XG improved the printability of the emulsion gel. After the XG concentration reached 2.0% (w/v), a stable structure with high resolution could be 3D printed. This study provides ideas for the utilization of *Hypsizygus marmoreus* by-products and the development of 3D printing PEG materials.

CRediT authorship contribution statement

Dan Xu: Methodology, Data curation, Writing – original draft, Writing – review & editing. **Xuebing Xing:** Methodology, Data curation, Writing – original draft. **Bimal Chitrakar:** Writing – review & editing. **Hongbo Li:** Methodology, Data curation. **Liangbin Hu:** Methodology, Data curation. **Jiayi Zhang:** Methodology, Data curation. **Xiaolin Zhu:** Methodology, Data curation. **Lishan Yao:** Methodology, Data curation. **Subrot Hati:** Writing – review & editing. **Zhenbin Liu:** Project administration, Supervision, Conceptualization, Funding acquisition. **Haizhen Mo:** Project administration, Supervision, Conceptualization, Funding acquisition.

Declaration of Competing Interest

The authors declare that they have no known competing financial interests or personal relationships that could have appeared to influence the work reported in this paper.

Data availability

Data will be made available on request.

Acknowledgements

The authors acknowledge the financial support from the National Key R&D Program of China (2021YFD1600400), National Natural Science Foundation of China (32101979), and Innovation Capability Support Program of Shaanxi Province (Program No. 2023-CX-TD-61) have enabled us to carry out this study.

References

An, Z., Liu, Z., Mo, H., Hu, L., Li, H., Xu, D., & Chitrakar, B. (2023). Preparation of Pickering emulsion gel stabilized by tea residue protein/xanthan gum particles and its application in 3D printing. *Journal of Food Engineering*.

Bi, A. Q., Xu, X. B., Guo, Y., Du, M., Yu, C. P., & Wu, C. (2022). Fabrication of flavour oil high internal phase emulsions by casein/pectin hybrid particles: 3D printing performance. *Food Chemistry*(Mar.1), 371.

Chang, Chao, Xue, Jingyi, Wang, Taoran, Luo, Yangchao, Zhou, & Mingyong. (2017). Pectin coating improves physicochemical properties of caseinate/zein nanoparticles as oral delivery vehicles for curcumin. *Food Hydrocolloids*.

Chen, S., Du, Y., Zhang, H., Wang, Q., Gong, Y., Chang, R., Zhang, J., Zhang, J., Yuan, Y., Liu, B., Yan, H., & Li, Y. (2022). The lipid digestion behavior of oil-in-water Pickering emulsions stabilized by whey protein microgels of various rigidities. *Food Hydrocolloids*.

Derkach, S. R. (2009). Rheology of emulsions. *Advances in Colloid and Interface Science, 151*(1–2), 1–23.

Dickinson, E. (2012). Emulsion gels: The structuring of soft solids with protein-stabilized oil droplets. *Food Hydrocolloids, 28*, 224–241.

Du, J., Dai, H., Wang, H., Yu, Y., & Zhang, Y. (2021). Preparation of high thermal stability gelatin emulsion and its application in 3D printing. *Food Hydrocolloids, 113*, Article 106536.

Girgih, A. T., Udenigwe, C. C., Li, H., Adebiyi, A. P., & Aluko, R. E. (2011). Kinetics of enzyme inhibition and antihypertensive effects of hemp seed (Cannabis sativa L.) protein hydrolysates. *Journal of the American Oil Chemists Society, 88*(11), 1767–1774.

Goldstein, N., & Reifen, R. (2022). The potential of legume-derived proteins in the food industry. *Grain & Oil Science and Technology, 5*(4), 167–178.

Hinderink, E. B. A., Schröder, A., Sagis, L. M. C., Schroën, K., & Berton-Carabin, C. C. (2021). Physical and oxidative stability of food emulsions prepared with pea protein fractions. *LWT*.

Huang, M., Wang, Y., Ahmad, M., Ying, R., & Tan, C. (2021). Fabrication of Pickering high internal phase emulsions stabilized by pecan protein/xanthan gum for enhanced stability and bioaccessibility of quercetin. *Food Chemistry,* (6), 129732.

Imeson, & Alan. (2009). Food Stabilisers, Thickeners and Gelling Agents. *Food Stabilisers Thickeners & Gelling Agents*.

Ingrid, Aguiló-Aguayo, Jennie, Walton, Inmaculada, Viñas, Brijesh, K., & Tiwari. (2017). Ultrasound assisted extraction of polysaccharides from mushroom by-products. *Lwt Food Science & Technology*.

Kaneko, T., Chihara, T., Shimpo, K., Beppu, H., & Sonoda, S. (2015). Inhibition of Azoxymethane-induced Colorectal Aberrant Crypt Foci in Mice Fed a High-fat Diet by Pleurotus eryngii (Eringi) and Hypsizygus marmoreus (Bunashimeji). *Asian Pacific Journal of Cancer Prevention Apjcp, 16*(9), 3881–3885.

Li, S., Huang, L., Zhang, B., Chen, C., & Huang, Q. (2020). Fabrication and characterization of starch/zein nanocomposites with pH-responsive emulsion behavior. *Food Hydrocolloids, 106341*.

Li, X., Fan, L., Liu, Y., & Li, J. (2021). New insights into food O/W emulsion gels: Strategies of reinforcing mechanical properties and outlook of being applied to food 3D printing. *Critical Reviews in Food Science and Nutrition*, 1–23.

Li, X., Liu, W., Xu, B., & Zhang, B. (2022). Simple method for fabrication of high internal phase emulsions solely using novel pea protein isolate nanoparticles: Stability of ionic strength and temperature. *Food Chemistry, 370*, Article 130899.

Lin, D., Kelly, A. L., & Miao, S. (2020). Preparation, structure-property relationships and applications of different emulsion gels: Bulk emulsion gels, emulsion gel particles, and fluid emulsion gels. *Trends in Food Science & Technology*.

Lin, J., Meng, H., Yu, S., Wang, Z., Ai, C., Zhang, T., & Guo, X. (2021). Genipin-crosslinked sugar beet pectin-bovine serum albumin nanoparticles as novel pickering stabilizer. *Food Hydrocolloids, 112*, Article 106306.

Liu, H., Xu, X. M., & Guo, S. D. (2007). Rheological, texture and sensory properties of low-fat mayonnaise with different fat mimetics. *LWT - Food Science and Technology, 40*(6), 946–954.

Liu, Y., Zhang, W., Wang, K., Bao, Y., & Zhou, P. (2019). Fabrication of Gel-Like Emulsions with Whey Protein Isolate Using Microfluidization: Rheological Properties and 3D Printing Performance. *Food and Bioprocess Technology* (1).

Liu, Z., Bhandari, B. R., Prakash, S., Mantihal, S., & Zhang, M. (2019). Linking rheology and printability of a multicomponent gel system of carrageenan-xanthan-starch in extrusion based additive manufacturing. *Food Hydrocolloids*.

Liu, Z., Bhandari, B. R., Prakash, S., & Zhang, M. (2018). Creation of internal structure of mashed potato construct by 3D printing and its textural properties. *Food Research International, 111*, 534–543.

Liu, Z., Zhang, M., Bhandari, B. R., & Wang, Y. (2017). 3D printing: Printing precision and application in food sector. *Trends in Food Science and Technology, 69*, 83–94.

Mezger, T. G. (2020). The Rheology Handbook: For users of rotational and oscillatory rheometers. *In*.

Millward, D. J. (2012). Amino acid scoring patterns for protein quality assessment. *The British Journal of Nutrition, 108*(Suppl 2), S31–S43.

Min, L., Wangjinsong, Y., Yongfa, Z., Hui, L., Jianjun, Z., & Le, J. (2018). Characterization, antioxidant and antiinflammation of mycelia selenium polysaccharides from Hypsizygus marmoreus SK-03. *Carbohydrate Polymers, 201*. S0144861718310087-.

Oliveira, R. S. B., Bellan, S. M. P., Viana, D. L., Di-Medeiros, S. R. F., Leal, M. C., Ana, F. D., … Carbonero, E. R. (2019). Structure elucidation of a bioactive fucomannogalactan from the edible mushroom Hypsizygus marmoreus. *Carbohydrate Polymers: Scientific and Technological Aspects of Industrially Important Polysaccharides, 225*.

Organization, W. H. (1991). Protein quality evaluation: report of the Joint FAO/WHO Expert Consultation, Bethesda, Md., USA, 4-8 December 1989. *Rome : FAO*.

Palazolo, G. G., Sobral, P. A., & Wagner, J. R. (2011). Freeze-thaw stability of oil-in-water emulsions prepared with native and thermally-denatured soybean isolates. *Food Hydrocolloids, 25*(3), 398–409.

Patel, A. R., Cludts, N., Sintang, M. D. B., Lesaffer, A., & Dewettinck, K. (2014). Edible oleogels based on water soluble food polymers: Preparation, characterization and potential application. *Food & Function, 5*.

Russ, N., Zielbauer, B. I., Ghebremedhin, M., & Vilgis, T. A. (2016). Pre-gelatinized tapioca starch and its mixtures with xanthan gum and ι-carrageenan. *Food Hydrocolloids, 56*(May), 180–188.

Shahbazi, H. E., & Rammile. (2021). Application of Pickering emulsions in 3D printing of personalized nutrition. Part I: Development of reduced-fat printable casein-based ink. *Colloids and Surfaces, A. Physicochemical and Engineering Aspects, 622*(1).

Shahbazi, M., Jaeger, H., & Ettelaie, R. (2022). A Promising Therapeutic Soy-Based Pickering Emulsion Gel Stabilized by a Multifunctional Microcrystalline Cellulose: Application in 3D Food Printing. *Journal of Agricultural and Food Chemistry, 7*, 70.

Sow, L. C., Chong, J. M. N., Liao, Q. X., & Yang, H. (2018). Effects of κ-carrageenan on the structure and rheological properties of fish gelatin. *Journal of Food Engineering, 239*(DEC.), 92–103.

Taha, A., Ahmed, E., Ismaiel, A., Ashokkumar, M., Xu, X., Pan, S., & Hu, H. (2020). Ultrasonic emulsification: An overview on the preparation of different emulsifiers-stabilized emulsions. *Trends in Food Science and Technology, 105*, 363–377.

Xing, X. B., Chitrakar, B., Hati, S., Xie, S. Y., Li, H. B., Li, C. T., … Mo, H. Z. (2022). Development of black fungus-based 3D printed foods as dysphagia diet: effect of gums incorporation. *Food Hydrocolloids, 123*.

Yu, J., Wang, X.-Y., Li, D., Wang, L., & Wang, Y. (2022). Development of soy protein isolate emulsion gels as extrusion-based 3D food printing inks: Effect of polysaccharides incorporation. *Food Hydrocolloids, 131*.

Zhang, J., Li, M., Li, C., & Liu, Y. (2019). Effect of wheat bran insoluble dietary fiber with different particle size on the texture properties,protein secondary structure,and microstructure of noodles. *Grain & Oil Science and Technology, 2*(4), 6.

Zhang, S. B., Jiang, Y., Zhang, S., & Chen, L. (2022). Physical Properties of Peanut and Soy Protein-Based Emulsion Gels Induced by Various Coagulants. *Gels, 8*.

Zong, Y., Kuang, Q., Liu, G., Wang, R., Feng, W., Zhang, H., Chen, Z., & Wang, T. (2022). All-natural protein-polysaccharide conjugates with bead-on-a-string nanostructures as stabilizers of high internal phase emulsions for 3D printing. *Food Chemistry* (Sep.15), 388.